

Modelling the engineering behaviour of fibrous peat formed due to rapid anthropogenic terrestrialization in Hangzhou, China

Item Type	Journal article
Authors	Yang, Z.X.;Zhao, C.F.;Cai, Y.Q.;Pan, K.;Wilkinson, Stephen;Zhao, C.F.
Citation	Yang, Z.X., Zhao, C.F., Cai, Y.Q., Pan, K., Xu, C.J., Wilkinson, S. (2016) 'Modelling the engineering behaviour of fibrous peat formed due to rapid anthropogenic terrestrialization in Hangzhou, China', Engineering Geology, 215, p.25-35
DOI	10.1016/j.enggeo.2016.10.009
Publisher	Elsevier
Journal	Engineering Geology
Download date	2026-05-15 04:45:01
License	https://creativecommons.org/licenses/by-nc-nd/4.0/
Link to Item	http://hdl.handle.net/2436/620292

1 **Modelling the engineering behaviour of fibrous peat formed due to rapid anthropogenic**
2 **terrestrialization in Hangzhou, China**

3
4 Z.X. Yang¹, C.F. Zhao², C.J. Xu³, S.P. Wilkinson⁴, Y.Q. Cai⁵, K. Pan⁶

5 **Abstract**

6 Peat is a very variable but normally weak material. While engineering failures involving peat
7 are common, the full diversity of engineering behaviours exhibited by peat have not been
8 well classified due to the large range of possible compositions of peats. A laboratory study
9 carried out on the peat at Jiangyangfan Eco-park, located in Hangzhou, China identify it as
10 displaying an intermediate engineering response compared to the ranges normally observed
11 for peat. The peat is a fill (made ground) originating from dredging of the West Lake, a site of
12 cultural and historic importance in China. Given its relatively unique mechanism of
13 deposition the distinctive characteristics of this peat are presented in comparison to other
14 peats reported in the literature highlighting its intermediate nature. The shearing behaviour
15 of peat can be described using the framework of critical state theory. The most prominent
16 characteristic of the West Lake Peat is that plastic deformation occurs at very small stress
17 levels. A constitutive model based on critical state theory for predicting the undrained shear
18 behaviour of this type of peat from low stress to critical state level is presented. This model
19 also includes several elements of peat behaviour previously reported and it may therefore

¹Professor, Dept. of Civil Engineering, Zhejiang University, China, zxyang@zju.edu.cn

²Former postgraduate student, Dept. of Civil Engineering, Zhejiang University, China, zhaochaofa@zju.edu.cn; currently
Ph.D student at Ecole Centrale de Nantes, France

³Professor, Dept. of Civil Engineering, Zhejiang University, China, xucj@zju.edu.cn

⁴Senior Lecturer, Department of Civil Engineering, University of Wolverhampton, Wulfruna Street, WV1 1LY, UK,
S.wilkinson4@wlv.ac.uk

⁵Professor, Department of Civil Engineering, Zhejiang University, caiyq@zju.edu.cn

⁶Postgraduate student, Dept. of Civil Engineering, Zhejiang University, China, pk2013@zju.edu.cn

20 be applied to a wider range of peat soils.

21 **Keywords:** Peat; physiochemical properties; compression; undrained shear; critical state;
22 constitutive model

23

24 **Introduction**

25 Peat is the most variable soil type with respect to engineering purposes. It is defined as a
26 predominantly organic soil which accumulates in-situ in a mire (BS 5930, 1999). However
27 peats and peaty soils can develop in a very wide range of geotechnical environments. In
28 addition to organic components, peats can contain the full range of constituents also found
29 in mineral soils depending on the conditions under which the peat has been formed. The
30 organic components of peat can also vary widely in terms of both origin and geotechnical
31 behaviour. In engineering peats are classified as ranging from fibrous peats, where the
32 organic constituents remain largely identifiable, to amorphous peats where the original
33 structure of the organic components have either been lost due to decomposition, or where
34 the peat was originally deposited as a sludge (BS EN ISO 14688-1, 2002). Within this broad
35 spectrum there is a large potential for variation in response to the range of organic
36 components from which the peat is formed. One of the more commonly used classification
37 systems for peat, presented by Hobbs (1986), uses twelve distinct scales for each of twelve
38 peat descriptors. Given all of the possible options within this system, a very large set of
39 unique peat classifications can be generated. While some combinations are unlikely in
40 practice, the term peat still encompasses a substantial range of materials with an equally
41 wide range of engineering behaviours. One of the most important factors controlling the

42 engineering behaviour of peat is the content of organic fibres. Fibres provide tensile strength,
43 and the amount of fibres in a peat is critical for its overall behaviour.

44 Peat is often described in the literature as a very soft and problematic engineering
45 material. Peats often have very high void ratio and water content, resulting in very low
46 initial values of bulk density. As a result peats often exhibit high values of compressibility,
47 and are commonly reported as responsible for excessive amounts of observed settlement
48 (Berry and Poskitt 1972, Edil et al 1991, Nichol and Farmer 1998, Mesri and Ajlouni 2007,
49 Kazemian et al 2011, Zhang and O’Kelly 2014). Many geotechnical structures such as slopes,
50 embankments, retaining walls and foundations which have been constructed on peat have
51 experienced damage or stability issues (Mesri and Choi 1985, Long 2005, Kværner and
52 Snilsberg 2008, Zwanenburg et al 2012, Boylan and Long 2014). In the majority of models for
53 simulating peat behaviour effective stress based approaches is commonly used directly
54 (Yamaguchi et al 1985, Long and Jennings 2006, den Haan and Grognet 2014). This approach
55 assumes that soil particles are incompressible. Peats have a high proportion of organic
56 particles which often have high intra-particle water contents. As these particles can
57 compress, deform and change their intra-particle moisture content the assumption of
58 incompressible particles is likely not valid. On this basis the applicability of the effective
59 stress based approach has recently been brought into question (Zhang and O’Kelly 2014).
60 When modelling peat engineering behaviour it is important to simulate its viscous nature
61 including its dependency on deformation rate and its long term deformation capacity.
62 Secondary consolidation in peat is often much more significant than for other geomaterials
63 (Mesri et al 1997, Kramer 2000, Mesri and Ajlouni 2007). In comparison to inorganic/clastic

64 soils, peats commonly display high values of undrained shear strength and much higher
65 effective friction angles (Yamaguchi et al 1985, Long 2005, Cheng et al. 2007, Mesri and
66 Ajlouni 2007, Hendry et al 2012, O’Kelly and Zhang 2013). This is especially true for peats
67 with a reasonably large quantity of constituent fibres or fragmented plant tissues.

68 A wide range of geotechnical materials have been successfully modelled using critical
69 state theory, but very few attempts to characterize peat using this approach have been
70 made. This is likely because samples are not sheared to critical state failure because samples
71 normally undergo tensile failure prior to reaching critical state due to the high frictional
72 strength of peat. However, recently effort has been made to understand peat behaviour
73 within the critical state framework. Boumezerane (2014) adopted a critical state based
74 kinematic model to simulate the unloading/reloading behaviour of peat, and den Han and
75 Feddema (2013) analysed the deformation and strength of embankments on soft Dutch peat
76 using a viscous version of the modified Cam-clay framework. These successes indicate that
77 there is a potential that critical state based approaches could be used to improve the
78 understanding of the engineering behaviour of peats and highly organic mineral soils. The
79 engineering behaviour observed from the peat samples, in addition to the range of
80 previously observed engineering behaviours of peats from across the world indicates the
81 range of behaviours that samples of peat can display.

82 This paper presents a laboratory study of the behaviour of peat obtained from the
83 Jiangyangfan Eco-park (originally dredged from the nearby West Lake) which is a wildlife
84 preserve within the city of Hangzhou, China. The West Lake peat is a fibrous material but
85 with a relatively low number of coarse fibres. A modified constitutive model based on a

86 critical state framework and concepts of dilatancy for simulating the undrained engineering
87 behaviour of this peat during shear failure is presented. Model applicability and accuracy is
88 evaluated by comparison with experimental results for the West Lake Peat sheared under
89 undrained conditions with varying initial consolidation stresses.

90

91 **Field site**

92 In 2008, the construction of an eco-park was initiated to develop the vacant Jiangyangfan
93 site (Fig. 1), 3km to the south of West Lake (also known as Xihu) near Hangzhou in Zhejiang
94 Province, China, as part of the West Lake Cultural Landscape, which was inscribed on
95 UNESCO's World Heritage List in 2011. Prior to 1999 the site was the Jiangyangfan reservoir,
96 however it was selected as the repository for materials dredged from the West Lake. The
97 West lake has been dredged by pipeline three times during its history in 1952, 1976 and
98 1999 respectively (Hangzhou local Chronicles compilation committee, 2003). Prior to this
99 date the lake had been dredged many times by hand during its history. In fact the first time
100 the lake is referred to in an official document using its current name West Lake ("Xihu") was
101 in relation to a request for dredging in the year 1090 by the famous poet Su Shi (1090), the
102 then governor of Hangzhou. This request refers to an even earlier dredging event performed
103 around year 821-824. Dredging of the lake is thus a major element of the local history and
104 culture. Prior to 1952 the lake had reached a very bad state with water depth reduced to
105 about 0.5m due to build-up of organic sludge. Leaves and vegetation had accumulated in the
106 lake along with clay and silt generating a material rich in organic matter at a very high
107 moisture content. It was then decided that the lake would undergo periodic dredging to

108 remove this sludge via temporary pipelines (Shao et al 2007). During the most recent
109 dredging carried out between 1999 and 2003 the sludge was excavated and pumped along
110 an approximately 4km long pipeline between West Lake and Jiangyangfan reservoir. During
111 transportation the sludge was mixed with large volumes of water, and thus its original fabric
112 was completely disrupted. During the four years of dredging approximately 1,000,000 m³ of
113 sludge was removed to Jingyangfan reservoir. The materials completely terrestrialized the
114 reservoir leaving only a few surface ponds of water between small hillocks of settling
115 dredged material. The peat at Jiangyangfan covers an area of over 100,000 m² and fills the
116 contours of the original reservoir going down to a depth of approximately 18m at the
117 deepest point (Fig. 2). After the completion of the dredging in 2003 the site was left
118 undisturbed during which time it underwent consolidation under its own self-weight until
119 2008 when construction of the Jiangyangfan Eco-park commenced. Fig. 3 shows aerial views
120 of Jiangyangfan Eco-park site during the period from 2000-2015.

121

122 Due to the difficult foundation conditions, construction of the main buildings took 2 years.
123 Across the rest of the park pedestrian walkways were constructed on floating footings. Some
124 covered pavilions and pagodas were built to allow tourists to observe birds and wildlife that
125 have colonised the wetland. At an early stage concerns were raised over the potential for
126 excessive settlement within the park, and so following construction the site was monitored;
127 at present settlements of over 700mm have been observed. The systematic experimental
128 investigation outlined below was carried out to better understand the causes of the
129 observed excessive settlement, to assist with remedial works on the current pedestrian

130 walkways and to aid the foundation design of future building/structures in and around the
131 eco-park.

132 Samples were obtained using a thin-wall sampler and taken to the laboratory for further
133 testing. The peat is known as West Lake Peat (WLP) as it was originally deposited within the
134 West Lake. Considering that the formation process of the WLP within Jiangyangfan Eco-park
135 is very different from the formation process followed by most other peat deposits, its basic
136 physical properties, mineral composition, micro-structure, and mechanical behaviour are all
137 presented. The tests outlined below were performed on reconstituted peat samples except
138 where specified.

139

140 **Peat mineralogy composition and index properties**

141 The WLP samples were dark brown and had a slight organic smell. The index and
142 physico-chemical properties of WLP are summarized in Table 1. The water content of the
143 peat was determined by oven-drying the specimens at a temperature of 65°C for 48 hours
144 following the National Standard of China (SSTE 1999) procedure. The initial water content w_0
145 of the natural peat varies in the range of 320-400%, whereas the reconstituted samples have
146 a mean initial water content w_0 of 182%. The ignition loss (N) was determined by
147 combustion at 700°C for 7 hours as suggested by SSTE (1999) giving an ignition loss of 35%.
148 Sempton and Petley (1970) suggested that organic matter content (OC) and loss on ignition
149 are approximately equivalent, such that the same values of N and OC are assumed for WLP
150 in this study.

151 As organic matter has a lower specific gravity G_s than most minerals, the specific gravity

152 (solids density) of peats and organic soils is usually less than those for inorganic soils
153 (2.65-2.76 g/cm³). The pycnometer method was used to determine the peats specific gravity,
154 and the mean value obtained was 2.12 g/cm³. G_s can be predicted from N using (den Haan
155 and Kruse 1986),

$$\frac{1}{G_s} = \frac{N}{1.354} + \frac{1-N}{2.746} \quad \text{Eq. (1)}$$

157 Substituting $N=0.35$ into above equation yields $G_s=2.02$, which is very close to the measured
158 value of 2.12 (Table 1). The permeability of peat is measured by a standard constant head
159 flow test using a permeameter (SSTE 1999) and is about 2.4×10^{-8} cm/s at a vertical load of σ'_v
160 =50 kPa and falls to 1.83×10^{-8} cm/s when σ'_v increases to 200 kPa.

161

162 **Classification of peat**

163 Two major systems exist for the classification of peat: the von Post (1922) system and the
164 Radforth (1969) system. At present both systems are widely used. From an engineering
165 perspective the von Post system has several advantages, its definition of the peats degree of
166 humification, which ranges from H_1 for intact, young peat to H_{10} for completely decomposed
167 peat, provides a good general idea of the state of the peat. The von Post system also
168 describes water content, and the content of fine and coarse fibres, wood and plant remnant,
169 all of which contribute towards the engineering behaviour of the peat. Hobbs (1986)
170 suggested that the von Post classification system should be further extended and so
171 proposed the modified von Post system through introducing categories for organic content,
172 anisotropy, tensile strength, odour, plasticity and acidity. This modified von Post
173 classification is very useful for engineering purposes because it covers most physical and

174 mechanical features of a peat and so this system was used during this study.

175 In the system extended by Hobbs (1986), each classifier is designated by a letter, and
176 the degree to which the characteristic is presented, is designated by an index. The rules for
177 classification presented in this paper are those of von Post (1922) and extended by Hobbs
178 (1986). Using this system, the WLP at Jiangyangfan Eco-park is classified as: B H₆ B₂ F₂ R₁ W₀
179 (von Post, 1922) / N₁ TV₂ TH₂ A₁ P₁ pH_L (extension proposed by Hobbs, 1986). This designates
180 the WLP as Bryales moss peat with a moderate degree of humification (H), water content
181 less than 500% (B), a high but not predominant fibre content (F), a low content of coarse
182 fibres (R), no wood (W), organic content 20% to 40% (N), moderate tensile strength in the
183 vertical direction (TV) and horizontal direction (TH), slight smell (A), a detectable plastic limit
184 (P) and acidity (pH).

185

186 **Microstructure**

187 An electron microscope investigation was carried out using a Hitachi TM 3000 tabletop
188 microscope to analyse the microstructure of the reconstituted WLP. The samples were
189 prepared by oven-drying, then they were mounted on 5mm aluminium stubs with double
190 sided sticky carbon tabs to ensure good conductivity between the sample and the stub. The
191 samples were then placed into the Scanning Electron Microscope (SEM). Samples were
192 imaged uncoated but at a relatively low vacuum to reduce the potential for charge build-up.
193 Some details of the SEM preparation techniques used for this peat are described in
194 Wilkinson (2011). Figures 4(a)-(f) are SEM micrographs of WLP. Fig. 4(a) shows the overall
195 nature of the microstructure of the WLP, being a mixture of plant fibre networks and

196 siliciclastic particles with some evidence of larger void spaces. The peat contains a few stem
197 structures (Fig. 4(b)-(d)) and decayed leaves on which a few stomal pores are visible as small
198 dimples in the leaf's otherwise smooth surface (Fig. 4(e)). In addition pyritic framboids were
199 observed in the soil suggesting relatively low oxygen concentrations within the peat (Fig.
200 4(f)). It is likely that the fibrous elements (Fig. 4(b-c)) could enhance the shear strength of
201 the peat especially as they are irregularly arranged (Fig. 4(d)).

202

203 **One-dimensional compression tests**

204 One dimensional compression tests were carried out to investigate the
205 consolidation/settlement behaviour of the WLP. Pichan and O'Kelly (2012) showed that the
206 compressional behaviour of peat depends on its degree of decomposition which relates to
207 the degree of humification within the von Post classification system outlined above. The
208 degree of decomposition of a peat is affected by environmental factors including
209 temperature, oxygen supply, pH, C:N ratio (carbon to nitrogen), and organic constituents, etc.
210 For the WLP the initial void ratio of the natural peat varies between 6.78 and 8.48 (Table 1),
211 and the reconstituted sample has a mean initial void ratio $e_0=3.86$. One-dimensional
212 compression tests were performed on reconstituted samples (20mm in height and 61.8mm
213 in diameter) using a conventional oedometer. A standard series of load increments were
214 employed for the test: 12.5kPa, 25kPa, 37.5kPa, 50kPa, 75kPa, 100kPa, 150kPa, 200kPa,
215 250kPa, 300kPa, 350kPa, 400kPa, 450kPa, 600kPa, and 800kPa. Each loading step lasted for
216 24 hours. Fig. 5(a) shows the cumulative axial strain with elapsed time for the first three
217 loading steps, and Fig. 5(b) shows the compression curve of the reconstituted peat sample.

218 Not surprisingly, the immediate compression is high, especially at high load levels, due to the
219 large void ratio and high compressibility. For the 25kPa and 50kPa loads, the immediate axial
220 strain is approximately 11% and 19%, which is much higher than the accepted settlement
221 limit for normal buildings or structures. At 50kPa, the total axial strain is about 28%. The
222 $e\text{-log}(\sigma_v)$ curves continue to decrease even after 24 hours (Fig. 5(a)), indicating a significant
223 amount of secondary consolidation. A linear trend is observed between void ratio e and
224 $\log(\sigma_v)$ when $\sigma_v > 12.5\text{kPa}$ (Fig. 5(b)), with a compression index of $c_c = 1.23$, identifying WLP as
225 highly compressible. The secondary compression index c_α is defined by the slope of the final
226 part of the compression curve, and is measured as the unit compression over one decade on
227 a log time scale, i.e. $c_\alpha = de/d\log(t)$. Based on a 24 hour standard oedometer test, the
228 measured mean c_α is about $0.07 \sim 0.10$ at $\sigma_v = 12.5\text{-}50\text{ kPa}$. The ratio of c_α/c_c represents the
229 deformability of soil particles. Peat deposits with highly deformable organic matter normally
230 have greater values for c_α/c_c , in comparison to granular media composed of less deformable
231 siliciclastic particles. The ratio of $c_\alpha/c_c = 0.056\text{-}0.081$ for the WLP compares well with the
232 normal expected range of 0.06 ± 0.01 for peat deposits given by Mesri et al (1997) and Mesri
233 and Ajlouni (2007). Mesri et al (1997) also observes that fibrous peats display the highest
234 c_α/c_c values of all geotechnical materials. The results from the fibrous WLP are, thus in full
235 agreement with this observation.

236

237 **Undrained triaxial compression tests**

238 Undrained triaxial tests were performed using a standard triaxial testing system, capable of
239 performing a variety of functions including isotropic and anisotropic consolidation and

240 various modes of shear loading. Reconstituted peat specimens were prepared and
241 consolidated using a specially designed consolidation apparatus for peat (Fig. 6). Large
242 inclusions including roots and pieces of gravel were removed before placing the peat into
243 the 150mm diameter 350mm height sample preparation acrylic tube. The sample was then
244 subjected to vertical compression under a confining stress of 30 kPa until a settlement rate
245 less than 0.005mm/hour was observed, which usually occurred after approximately 120
246 hours. The compressed sample was pushed out of the tube and trimmed to a length of
247 140mm and a diameter of 70mm for consolidated undrained (CU) triaxial testing. In total,
248 five reconstituted specimens were prepared at initial effective confining stresses ranging
249 from 30 to 200 kPa.

250 A back pressure of 200 kPa was applied to all CU test specimens to achieve full
251 saturation, which was confirmed by checking that the Skempton B values were greater than
252 0.98. The specimens were then isotropically consolidated to the desired value of confining
253 pressure and then a strain controlled undrained triaxial shear test was conducted at a speed
254 of 3% strain per hour. As suggested by Jardine (2013), ageing periods were imposed during
255 the consolidation stage prior to the samples being sheared. During each step, the residual
256 creep rates were reduced to <1% of those that would be developed in the shearing stage. As
257 a result, each sample was consolidated for about 6 days before being sheared to critical
258 state which occurred at a strain of 20% for triaxial compression. The axial load was
259 measured using a load cell and the axial displacement was measured using a linear variable
260 differential transformer (LVDT).

261 Fig. 7 summarizes the results of CU triaxial tests on reconstituted peat specimens. The

262 specimens display predominately strain-hardening behaviour up to large deformations (Fig.
263 7(a)), with the exception that slight strain-softening responses were observed for the higher
264 initial effective stresses $p'_0=100$ and 200 kPa. In $q-p'$ stress space (Fig. 7(b)), the undrained
265 contractive behaviour is primarily seen from the increase in q during strain-hardening
266 accompanied by a decrease in p' for all specimens. It is also noted that during the later stage
267 of shearing, all specimens exhibit apparent volumetric dilation after passing through the
268 phase transformation state, where the peats behaviour changes from 'contraction' to
269 'dilation' as is normally observed in sand samples (Ishihara et al 1975). To assist in defining
270 the failure behaviour, the 'tension cut-off' with an inclination $q/p'=3$ through the origin is
271 also plotted in the $q-p'$ plane, which signifies a zero effective stress condition. The stress
272 paths are all below this line, indicating that no tensile failure occurs for the WLP samples.
273 Critical state failure is identified for these specimens when the axial strain ϵ_a reaches
274 approximately 20% (Fig. 7(a)). 'Tension cut-off' failures under triaxial compression are
275 commonly observed in peat, especially for fibrous peat samples (den Hann and Kruse 2007,
276 Mesri and Ajlouni 2007, Zwanenburg et al. 2012). The lack of a 'tension cut-off' failure in the
277 WLP is possibly due to the relatively low fibre content in the WLP (35%) in comparison to
278 other peats. Although some fibres may break in tension, the frictional shear component
279 controls the overall engineering behaviour of this fibrous peat. This type of behaviour is also
280 observed by Yamaguchi et al. (1985) and Cola and Cortellazzo (2005). This suggests that the
281 content and type of organic fibres will determine the failure mechanism and behaviour of
282 fibrous peats during engineering works.

283 The critical state of the peat is approximated by the state of the specimens at 20% axial

284 strain at which the rate of change of effective mean normal stress and deviatoric stress
285 becomes insignificant (Fig. 7). The estimated critical state can be represented by the critical
286 state lines (CSL) in a $q-p'$ plane and an $e-\log p'$ plane, as shown in Fig. 8 (a) and (b)
287 respectively. In the $q-p'$ plane (Fig. 8(a)), the soil approaches a unique CSL regardless of its
288 initial states. The critical stress ratio is 1.948, giving a critical state friction angle of 47.3° ,
289 which is much higher than those for mineral soils due to the shear resistance caused by
290 organic fibres. Similar observations have been reported by Yamaguchi et al (1985), Long
291 (2005), Mesri and Ajlouni (2007), Hendry et al (2012), O'Kelly and Zhang (2013). In Fig. 8(b),
292 the critical state points can be fitted onto a straight line with a slope of 1.225. The initial
293 states of shearing after isotropic consolidation are also shown in this figure, and they can be
294 fitted onto an isotropic consolidation line (ICL) with a slope of 1.139.

295 The WLP has a distinctive effective stress path in the $q-p'$ plane. From a very early stage
296 of shearing with small stress ratios q/p' , p' decreases due to the build-up of pore water
297 pressure (Fig. 7(b)), leading to an inclined effective stress path on which the tangential line
298 of the effective stress path at $p'=0$ is not vertical. Similar observations are also reported by
299 Yamaguchi et al (1985), Cola and Cortellazzo (2005), Cheng et al (2007), Hendry et al (2012),
300 and Zwanenburg et al. (2012). This suggests plastic deformation could occur for fibrous
301 peats like WLP at very small stress ratios. In the conventional framework of elastoplasticity,
302 the slope of the initial effective stress path in the $p'-q$ plane can be employed to identify the
303 elastic or elastoplastic response of materials. If the soil exhibits purely elastic behaviour
304 under undrained conditions, the $d\varepsilon_v^p = 0$, and thus $d\varepsilon_v^e = 0$ as $d\varepsilon_v = d\varepsilon_v^e + d\varepsilon_v^p = 0$; then
305 $d\varepsilon_v^e = dp' / K = 0$, where $d\varepsilon_v$ is the volumetric strain increment with superscripts 'e' and 'p'

306 signifying elastic and plastic and K is bulk modulus, and therefore no change of p' occurs,
307 resulting in the tangential line of the effective stress path at $p'=0$ being perpendicular to the
308 p' axis. This type of effective stress path is observed in undrained triaxial compression shear
309 test on both sands and normally consolidated clays (Fig. 9), which is confirmed by the small
310 strain behaviour of clays and sands investigated extensively with high-resolution triaxial
311 experiments by Vucetic and Dobry (1988, 1991), Smith et al. (1992), Kuwano and Jardine
312 (2007). Some peats, reported in the literature also display purely elastic behaviour at small
313 stress ratios similar to the behaviour of mineral soils, e.g. those reported by Long (2005),
314 den Haan and Kruse (2007), Mesri and Ajlouni (2007). The reason for these two distinctive
315 behaviours for different peats at very small stress ratios is related to the composition of the
316 peats. The exact elements of the peats which cause this have not been fully understood.
317 However, this again highlights the range of compositions of peat soils which generates the
318 range of observed engineering behaviours.

319 To further verify that plastic deformation occurs in the WLP occurring at the start of
320 shearing, cyclic undrained triaxial compression tests with low amplitudes $q_{cyc}=5$ kPa and
321 $p'_0=50$ kPa were performed with both Toyoura sand and the WLP samples. The loading
322 programme is shown in Fig. 10(a). Fig. 10(b) compares the stress paths of peat and sand in
323 the first loading cycle. As expected, the stress path for the sand is almost vertical in the first
324 cycle without generating any pore pressure, in comparison the WLP is not vertical, with a net
325 pore pressure of 5 kPa generated in the first cycle. Fig. 10(c) presents the accumulative axial
326 strains in the first cycle. Nearly 0.06% axial strain takes place in the first cycle for the WLP,
327 while no discernable strain is produced for the sand. Similar observations are confirmed by

328 dynamic triaxial tests on peats at small strain carried out by Boulanger et al. (1998), Kramer
329 (2000), Wehling et al. (2003), in which purely elastic, linear and non-hysteretic responses
330 were not observed, even at extremely small stress/strain levels, such as would be seen in
331 other siliciclastic soils. This behaviour of the peat forms one of the key elements of the
332 constitutive model presented in the following section.

333

334 **A simple triaxial compression model**

335 During the last several decades, critical-state soil mechanics (Schofield and Wroth 1968) has
336 been extensively used to model the behaviours of both sand and clay (Li and Dafalias 2000;
337 Ling and Yang 2006; Kaliakin and Dafalias 1990; Schofield and Wroth 1968). For example, Li
338 and Dafalias (2000) proposed a state-dependent dilatancy model for sand, which is capable
339 of describing sand behaviour at different initial densities and under different initial confining
340 pressures with a single set of model constants. Given the advantage of Li and Dafalias' model,
341 it was adopted to simulate the undrained triaxial compression behaviour of WLP.

342 The critical state line in the e - p' plane can be expressed as (Li and Wang 1998)

$$343 \quad e_c = e_r - \lambda_c (p' / p_a)^\xi \quad \text{Eq. (2)}$$

344 where e_c is the critical state void ratio corresponding to p' , and e_r , λ_c and ξ are three material
345 constants for critical state line. Using this equation, the state parameter ψ proposed by Been
346 and Jefferies (1985) can be obtained as

$$347 \quad \psi = e - e_c \quad \text{Eq. (3)}$$

348 where e is the void ratio at the current state. The sign of ψ can be used to determine the
349 state of the soil considering the influence of both density and pressure (Been and Jefferies

350 1985; Li and Dafalias 2000).

351 As shown in Fig. 7, the critical state of the WLP is approximated by the state of the
352 specimens at approximately 20% axial strain at which the rate of change of both deviatoric
353 and mean normal effective stresses becomes insignificant. Under undrained conditions, it is
354 assumed that plastic deformation can only occur when the stress ratio $\eta=q/p'$ exceeds its
355 historic maxima for virgin loading, and no plastic deformation will be produced along a
356 constant η stress path. This assumption is approximately true for sand, as no significant
357 volume change is induced for a constant stress ratio η under normal confining stress levels,
358 before particle breakage occurs. However, for clay and peat, considerable volumetric
359 deformation is observed due to consolidation, and thus the plastic deformation which
360 occurs along a constant η stress path cannot be neglected. In this study, given that only
361 undrained triaxial tests were performed, no yielding occurs due to increases in p' . Thus this
362 assumption is still valid. The yield criterion can be written as (Li and Dafalias 2000)

$$363 \quad f = q - \eta p' = 0 \quad \text{Eq. (4)}$$

364 The condition of consistency of the yield function of Eq. (4) can be expressed as:

$$365 \quad df = \frac{\partial f}{\partial p'} dp' + \frac{\partial f}{\partial q} dq - \langle L \rangle K_p = 0 \quad \text{Eq. (5)}$$

366 in which K_p is the plastic modulus and L is the loading index defined as

$$367 \quad L = \frac{1}{K_p} \left(\frac{\partial f}{\partial p'} dp' + \frac{\partial f}{\partial q} dq \right) = \frac{dq - \eta dp'}{K_p} = \frac{p' d\eta}{K_p} \quad \text{Eq. (6)}$$

368 An associated flow rule is applied in deviatoric space, such that

$$369 \quad d\varepsilon_q^p = \langle L \rangle \frac{\partial f}{\partial q} = p' d\eta / K_p \quad \text{Eq. (7)}$$

370 where $\langle \rangle$ is the Macauley bracket such that $\langle L \rangle = L$ for $L > 0$ and $\langle L \rangle = 0$ when $L \leq 0$.

371 By applying a dilatancy relation, the plastic volumetric strain increment can be written as

$$372 \quad d\varepsilon_v^p = Dd\varepsilon_q^p = D\langle L \rangle \frac{\partial f}{\partial q} = Dp' d\eta / K_p \quad \text{Eq. (8)}$$

373 Where, the following dilatancy function is proposed,

$$374 \quad D = d_0(e^{m\psi} - \sqrt{\eta/M}) \quad \text{Eq. (9)}$$

375 In which d_0 and m are two material constants for the dilatancy equation and M is the critical
376 stress ratio. Eq. (9) is slightly different from the one employed by Li and Dafalias (2000) for
377 fine tuning the performance of their model. It can be seen that at the critical state, $\psi=0$ and
378 $\eta=M$, the dilatancy D is zero according to Eq. (9), which satisfies the requirement for the
379 critical state. More importantly, this equation can also describe both positive and negative
380 dilatancy, depending on the state of the soils which is characterized by the state parameter
381 ψ .

382 The elastic strain increments can be obtained through linear elasticity as

$$383 \quad d\varepsilon_v^e = dp' / K \quad \text{and} \quad d\varepsilon_q^e = dq / 3G \quad \text{Eq. (10)}$$

384 in which $d\varepsilon_v^e$ and $d\varepsilon_v^p$ are elastic and plastic strain increments respectively; G and K denote
385 the elastic shear and bulk moduli respectively. As the elastic properties of soils are normally
386 pressure sensitive, G can be expressed by an empirical formula as follows,

$$387 \quad G = G_0 F(e) (p' / p_a)^{0.5} \quad \text{Eq. (11)}$$

388 in which G_0 is a dimensionless material constant and can be determined by resonant column
389 tests; p_a is the atmospheric pressure for normalization; $F(e)$ is a function of the current void
390 ratio e with a typical form of (Hardin and Richart 1963; Richart et al 1970; Iwasaki and
391 Tatsuoka 1977)

392
$$F(e) = \frac{(2.97 - e)^2}{1 + e} \quad \text{Eq. (12)}$$

393 The bulk modulus K can be expressed as

394
$$K = G \frac{2(1 + \nu)}{3(1 - 2\nu)} \quad \text{Eq. (13)}$$

395 where ν is Poisson's ratio of soils and for simplicity, can be treated as a material constant
396 independent of the pressure.

397 Noting the additive decomposition of the strains $d\varepsilon_v = d\varepsilon_v^e + d\varepsilon_v^p$ and $d\varepsilon_q = d\varepsilon_q^e + d\varepsilon_q^p$, and
398 by combing Eqs. (7) - (9), we can obtain the incremental stress-strain relation in triaxial
399 space,

400
$$\begin{Bmatrix} dq \\ dp' \end{Bmatrix} = \Lambda \begin{Bmatrix} d\varepsilon_q \\ d\varepsilon_v \end{Bmatrix} \quad \text{Eq. (14)}$$

401 where Λ is the elastoplastic stiffness matrix and can be explicitly expressed as

402
$$\Lambda = \left[\begin{pmatrix} 3G & 0 \\ 0 & K \end{pmatrix} - \frac{h(L)}{K_p + 3G - K\eta D} \begin{pmatrix} 9G^2 & -3KG\eta \\ 3KGD & -K^2\eta D \end{pmatrix} \right] \quad \text{Eq. (15)}$$

403 where $h(L)$ is the Heaviside step function, with $h(L > 0) = 1$ and $h(L \leq 0) = 0$.

404 The plastic modulus is defined to capture the hardening and softening of soil responses
405 under shear loading. Given the lack of information from observed plastic hardening
406 behaviour associated with microstructural evolution, the plastic modulus K_p can also be
407 defined as a function of the stress ratio η and state parameter ψ ,

408
$$K_p = Gh(M - \eta e^{n\psi}) = Ghe^{-m\psi} (Me^{m\psi} - \eta) \quad \text{Eq. (16)}$$

409 where h and n are two positive model constants; the elastic modulus G serves as a reference,
410 rendering h dimensionless. Eq. (16) is a modified version of that employed for modelling
411 sands by Li and Dafalias (2000), which is intended to model the exact response at stress ratio

412 $\eta=0$. It is seen that Eq. (16) inherits the merits of its original form for sand. For example, at
413 the critical state, $\psi=0$ and $\eta=M$, which result in $K_p=0$, such that $d\eta / d\varepsilon_q^p = 0$, which coincides
414 with the condition of perfect plastic flow at the critical state. In addition: 1) K_p can be
415 positive or negative, depending on the value of ψ , such that it can describe a hardening or
416 softening response during shearing; 2) K_p used by Li and Dafalias (2000) will become infinite
417 when $\eta=0$, indicating that no plastic deviatoric strain occurs, nor is there any plastic
418 volumetric strain. This holds true for most normally consolidated soils, which have a purely
419 elastic response with a non-zero, small $d\eta$ at $\eta=0$, resulting in $d\varepsilon_q^p = 0$ and such that $d\varepsilon_v^p = 0$.
420 $d\varepsilon_q^p = 0$ yields an isotropic deformation, while $d\varepsilon_v^p = 0$ suggests that the tangent of the
421 effective stress path in the q - p' will be vertical, and no change in the effective p' is allowed to
422 take place under undrained conditions. However, for WLP, the effective stress path bends
423 towards the reduction in effective stress p' right from the starting point at $\eta=0$ (Fig. 7b), and
424 there is no purely elastic zone as discussed before.

425 The model variable h in Eq. (16) is found to be void ratio (e)-dependent, and a simple
426 linear relation is proposed by Li and Dafalias (2000) as

$$427 \quad h = h_1 - h_2 e \quad \text{Eq. (17)}$$

428 where h_1 and h_2 are two material constants. Eq. (18) has integrated the influence of the soil
429 density over a wide range of variation. As noted by Li (2002), an e -dependent function is
430 used rather than a ψ -dependent function, because a change either in e or p' will alter ψ ,
431 while the influence of p' has been accounted for by the elastic shear modulus G in Eq. (11).

432

433 **Model calibration and responses**

434 In total, 11 material constants should be calibrated and used in this model. These constants
435 can be grouped into four categories (Table 2) according to their functions. The critical stress
436 ratio M is obtained by fitting the results of triaxial compression tests in the $q-p'$ plane in Fig.
437 7(a). Parameters e_r , λ_c , and ξ are determined by fitting the test data with linearization of the
438 critical state line in the $e-p'$ plane with Eq. (2), which is shown in Fig. 11 (Li and Wang 1998).
439 The elastic, dilatancy and hardening parameters can be calibrated and adjusted finely to fit
440 the test data, using the calibration procedure described in Li and Dafalias (2000). All
441 resulting constants are presented in Table 2.

442 In general, the model simulations compare well with the experimental results (Fig. 12).
443 the model is able to simulate the response of WLP at low stress ratio levels, where the
444 effective stress paths bend towards the reduction of the effective stresses in the $q-p'$ plane
445 (Fig. 12(a)). The model can also capture the stress-strain responses from small strain levels
446 up to the critical state (Fig. 12(b)). Slight discrepancies are observed at very low strain levels.
447 These are probably related to the uncertainties associated with the accurate measurement
448 of the true small strain behaviour of undisturbed peat, and the uncertain behaviour of
449 deformable organic particles at these small strains.

450

451 **Conclusions**

452 The following five main conclusions flow from the work described above:

- 453 1. The West Lake Peat (WLP) investigated in this study is similar in many ways to typical
454 peats: it has a relatively high water content and low bulk density, it is highly
455 compressible and its secondary compression is significant. However, although the fibre

456 content of WLP is significant it is not dominant.

- 457 2. The undrained shear behaviour of WLP can be described using critical state theory. No
458 'tension cut-off' failure was observed prior to occurrence of critical state failure, which is
459 primarily due to its relatively low fibre content. In addition, the WLP has a higher critical
460 state friction angle of approximately 47.3° , which is much higher than those of mineral
461 soils and is normally caused by the reinforcing effect of fibres in peats.
- 462 3. The most prominent observation of the WLP is that plastic deformation occurs at very
463 small stress levels. The feature is very similar to the behaviour of many peats worldwide,
464 while most mineral soils behave elastically under similar low stress ratios.
- 465 4. A constitutive model is presented that has simulative capability in predicting the
466 undrained shear behaviour. The model response compares well with the experimental
467 results from the beginning of shearing through to critical state failure.
- 468 5. Given that the WLP has intermediate behaviour in comparison to other peats, this model
469 has sufficient flexibility to describe the behaviour of a wide range of peats.

470

471 The results of this study provide a fundamental basis for understanding the engineering
472 behaviour of the WLP in Jiangyangfan Eco-park. It has been used to inform the remedial
473 works for existing structures and foundation works for future buildings/structures in the
474 park. At the broader scale this work provides another case study of the behaviour of a peat
475 and highlights the wide variety of potential behaviours of this diverse and variable
476 geotechnical material.

477

478 **Acknowledgments**

479 The research described was funded by the Natural Science Foundation of China (Grant Nos.
480 51322809, 51578499), Qianjiang Manage Office of Hangzhou Administration Bureau of
481 Gardens, the National Key Basic Research Program of China (No. 2015CB057801). Their
482 support is gratefully acknowledged. Gratitude is also extended to Dr XS Li, for insightful
483 discussions and constructive comments on the constitutive modelling of peat.

484

485 **References**

486 Been, K., and Jefferies, M.G. (1985). A state parameter for sands. *Géotechnique*, 35(2),
487 99-112.

488 Berry, P.L., and Poskitt, T. J. (1972). The consolidation of peat. *Géotechnique*, 22(1), 27-52.

489 British Standards Institution, 1999. Code of practice for site investigation, BS 5930:1999. Her
490 Majesty's Stationary Office, London.

491 British Standards Institution, 2002. Geotechnical investigation and testing — Identification
492 and classification of soil, BS EN ISO 14688-1: 2002. Her Majesty's Stationary Office,
493 London.

494 Boulanger, R.W., Arulnathan, R., Harder, L.F.Jr., Torres, R.A., and Driller, M.W. (1998). Dynamic
495 properties of Sherman Island peat. *Journal of Geotechnical and Geoenvironmental*
496 *Engineering*, 124(1), 12-20.

497 Boumezerane, D. (2014). Modeling unloading/reloading in peat using a kinematic bubble
498 model. *Numerical Methods in Geotechnical Engineering*, Hick, Bringreve & Rohe (Eds),
499 Taylor & Francis Group, London, 1, 9-14.

500 Cheng, X.H., Ngan-Tillard, D.J.M., and den Haan, E.J. (2007). The causes of the high friction
501 angle of Dutch organic soils. *Engineering Geology*, 93(1), 31-44.

502 Cola, S., and Cortellazzo, G. (2005). The shear strength behaviour of two peaty soils.
503 *Geotechnical and Geological Engineering*, 23(6), 679-695.

504 den Haan, E.J., and Kruse, G.A.M. (2007). Characterisation and engineering properties of
505 Dutch peats. In *Proceedings of the Second International Workshop of Characterisation
506 and Engineering Properties of Natural Soils*, Singapore, 29, 2101-2133.

507 den Haan, E.J., and Grognet, M. (2014). A large direct simple shear device for the testing of
508 peat at low stresses, *Géotechnique Letters*, 4, 283-288.

509 den Haan, E.J., and Feddema, A. (2013). Deformation and strength of embankments on soft
510 Dutch soil, *Proceedings of the ICE-Geotechnical Engineering*, 166(GE3), 239-252.

511 Edil, T.B., Fox, P.J., and Lan, L.T. (1991). Observational procedure for settlement of peat. *Proc.*
512 *Geo-Coast*, 91, 165-170.

513 Hangzhou local Chronicles compilation committee (2003). *Chronicles of Hangzhou*.
514 <http://www.hangzhou.gov.cn/main/zjhz/hzsz/index.jsp> (in Chinese).

515 Hardin, B.O., and Richart, F.E. (1963). Elastic wave velocities in granular soils. *Journal of Soil*
516 *Mechanics and Foundations Division*, ASCE, 89(SM1), 39-56.

517 Hendry, M.T., Sharma, J.S., Martin, C.D., & Barbour, S.L. (2012). Effect of fibre content and
518 structure on anisotropic elastic stiffness and shear strength of peat. *Canadian*
519 *Geotechnical Journal*, 49(4), 403-415.

520 Hobbs, N.B. (1986) Mire morphology and the properties and behaviour of some British and
521 foreign peats. *Quart. J. of Eng. Geol.*, 19: 7-80.

522 Ishihara K., Tatsuoka F., and Yasuda S. (1975). Undrained deformation and liquefaction of
523 sand under cyclic stresses. *Soils Foundations*, 15(1), 29–44.

524 Iwasaki, T., and Tatsuoka, F. (1977). Effects of grain size and grading on dynamic shear moduli
525 of sand. *Soils and Foundations*, 17(3), 19-35.

526 Jardine, R.J. (2013). Advanced laboratory testing in research and practice. 2nd Bishop
527 Lecture, 18th Conf. on Soil Mechanics and Geotechnical Engineering, Publisher: Presses
528 des Ponts, 25-55.

529 Long, M. (2005). Review of peat strength, peat characterisation and constitutive modelling
530 of peat with reference to landslides. *Studia Geotechnica et Mechanica*, 27(3-4), 67-90.

531 Kaliakin, V., and Dafalias, Y.F. (1990). Theoretical aspects of the elastoplastic-viscoplastic
532 bounding surface model for cohesive soils. *Soils and Foundations*, 30(3), 11–24.

533 Kazemian, S., B.K. Huat, B.B.K., Prasad, A. and Barghchi, M. (2011). A state of art review of
534 peat: Geotechnical engineering perspective. *International Journal of the Physical
535 Sciences*, 6(8), 1974-1981.

536 Kramer, S.L. (2000). Dynamic response of Mercer Slough peat. *Journal of Geotechnical and
537 Geoenvironmental Engineering*, 126(6), 504-510.

538 Kuwano, R., and Jardine, R.J. (2007). A triaxial investigation of kinematic yielding in sand.
539 *Géotechnique*, 57(7), 563-579.

540 Kværner, J., and Snilsberg, P. (2008). The Romeriksporten railway tunnel-drainage effects on
541 peatlands in the lake Northern Puttjern area. *Engineering Geology*, 101(3), 75-88.

542 Long, M., and Jennings, P. (2006). Analysis of the peat slide at Pollatomish, County Mayo,
543 Ireland. *Landslides*, 3, 51–61.

544 Li, X.S. (2002). A sand model with state-dependent dilatancy. *Géotechnique*, 52(3), 173-186.

545 Li, X.S., and Dafalias, Y.F. (2000). A sand model with state-dependent dilatancy.
546 *Géotechnique*, 50(4), 449-460.

547 Li, X.S., and Wang, Y. (1998). Linear representation of steady-state line for sand. *Journal of*
548 *Geotechnical and Geoenvironmental Engineering*, 124(12), 1215-1217.

549 Ling, H. I., and Yang, S. (2006). Unified sand model based on the critical state and generalized
550 plasticity. *Journal of Engineering Mechanics*, 132(12), 1380–1391.

551 Mesri, G., and Ajlouni, M. (2007). Engineering properties of fibrous peats. *Journal of*
552 *Geotechnical and Geoenvironmental Engineering ASCE*, 133(7), 850-866.

553 Mesri, G., and Choi, Y.K. (1985). Settlement analysis of embankments on soft clays. *Journal*
554 *of Geotechnical Engineering*, 111(4), 441-464.

555 Mesri, G., Stark, T.D., Ajlouni, M.A., and Chen, C.S. (1997). Secondary compression of peat
556 with or without surcharging. *Journal of Geotechnical and Geoenvironmental*
557 *Engineering*, 123(5), 411-421.

558 Nichol, D., and Farmer, I.W. (1998). Settlement over peat on the A5 at Pant Dedwydd near
559 Cerrigydrudion, North Wales. *Engineering Geology*, 50(3), 299-307.

560 O'Kelly, B.C., and Zhang, L. (2013). Consolidated-drained triaxial compression testing of peat.
561 *ASTM Geotechnical Testing Journal*, 36(3), 310-321.

562 Pichan, S.P. and O'Kelly, B.C. (2012). Effect of decomposition on the compressibility of fibrous
563 peat, *ASCE GeoCongress 2012: State of the Art and Practice in Geotechnical*
564 *Engineering*, Oakland, California, USA, 25th–29th March, 2012, edited by R.D. Hryciw, A.
565 Athanasopoulos-Zekkos and N. Yesiller, (GSP 225), 4329 – 4338.

566 Pichan, S.P., and O'Kelly, B.C. (2012). Stimulated decomposition in peat for engineering
567 applications. *Proceedings of the ICE-Ground Improvement*, 166(3), 168-176.

568 Radforth, N.W. (1969). Classification of muskeg. In: MacFarlane, I. C. (ed.) *Muskeg*
569 *engineering handbook*. Canadian Building Series. University of Toronto Press.

570 Richard, F.E., Hall, J.R., Woods, R.D. (1970). *Vibrations of soils and Foundations*. Prentice-Hall:
571 Englewood Cliffs, NJ, 1970.

572 Schofield, A.N., and Wroth, C.P. (1968). *Critical state soil mechanics*, McGraw Hill, London

573 Shao, Y.F., He, C., Lou, Q.Q. (2007). Stabilization of dredged silt from West Lake. *Journal of*
574 *Jiangsu University (Natural Science Edition)*, 28(5), 442-445. (in Chinese).

575 Shu, S. (1090). The request of dredging West Lake in Hangzhou.
576 http://blog.sina.com.cn/s/blog_500bc46501012fe3.html, in Chinese.

577 Skempton, A. W., & Petley, D. J. (1970). Ignition loss and other properties of peats and clays
578 from Avonmouth, King's Lynn and Cranberry Moss. *Géotechnique*, 20(4), 343-356.

579 Smith, P.R., Jardine, R.J., and Hight, D.W. (1992). The yielding of Bothkennar clay.
580 *Géotechnique*, 42(2), 257-274.

581 Standard for Soil Test Method (SSTE 1999). National Standard of the People's Republic of
582 China, GB/T50123-1999. China Planning Press, October 1999.

583 Wehling, T.M., Boulanger, R.W., Arulnathan, R., Harder, L.F. Jr, and Driller, M.W. (2003).
584 Nonlinear dynamic properties of a fibrous organic soil. *Journal of Geotechnical and*
585 *Geoenvironmental Engineering*, 129(10), 929-939.

586 Wilkinson, S. (2011). *The Microstructure of UK Mudrocks*, PhD thesis, Department of Civil
587 and Environmental Engineering, Imperial College London.

588 von Post, L. (1922) Sveriges Geologiska Undersoknings torvinventering och nogra av dess
589 hittils vunna resultat (SGU peat inventory and some preliminary results). Svenska
590 Mosskulturforeningens Tidskrift, Jonkoping, Sweden, 36, 1-37.

591 Vucetic, M., and Dobry, R. (1988). Degradation of marine clays under cyclic loading. Journal
592 of Geotechnical Engineering, 114(2), 133-149.

593 Vucetic, M., and Dobry, R. (1991). Effect of soil plasticity on cyclic response. Journal of
594 Geotechnical Engineering, 117(1), 89-107.

595 Yamaguchi, H., Ohira, Y., Kogure, K., and Mori, S. (1985). Undrained shear characteristics of
596 normally consolidated peat under triaxial compression and extension conditions. Soils
597 and foundations, 25(3), 1-18.

598 Zhang, L., and O'Kelly, B.C. (2014). The principle of effective stress and triaxial compression
599 testing of peat. Proceedings of the ICE-Geotechnical Engineering, 167(GE1), 40-50.

600 Zwanenburg, C., den Haan, E.J., Kruse, G.A.M., and Koelewijn, A.R. (2012). Failure of a trial
601 embankment on peat in Booneschans, the Netherlands. Géotechnique, 62(6), 479-490.

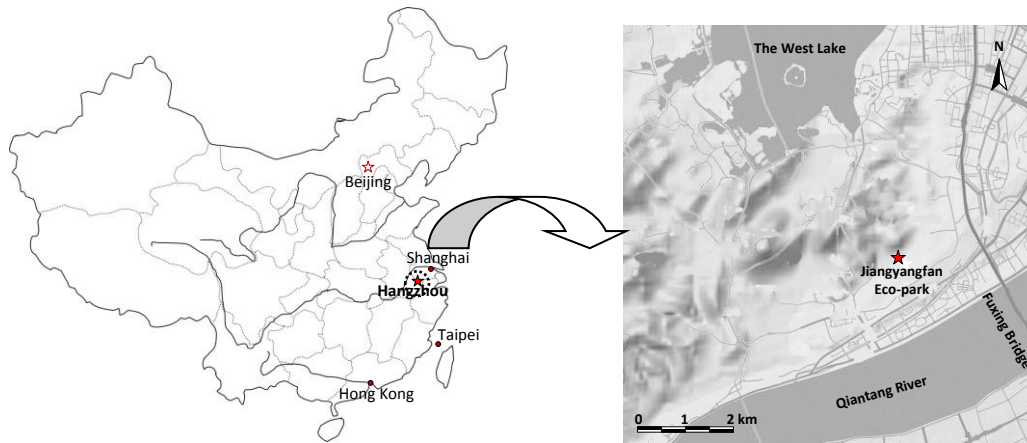


Fig. 1 Maps showing sites of West Lake in Hangzhou and Jiangyangfan Eco-park

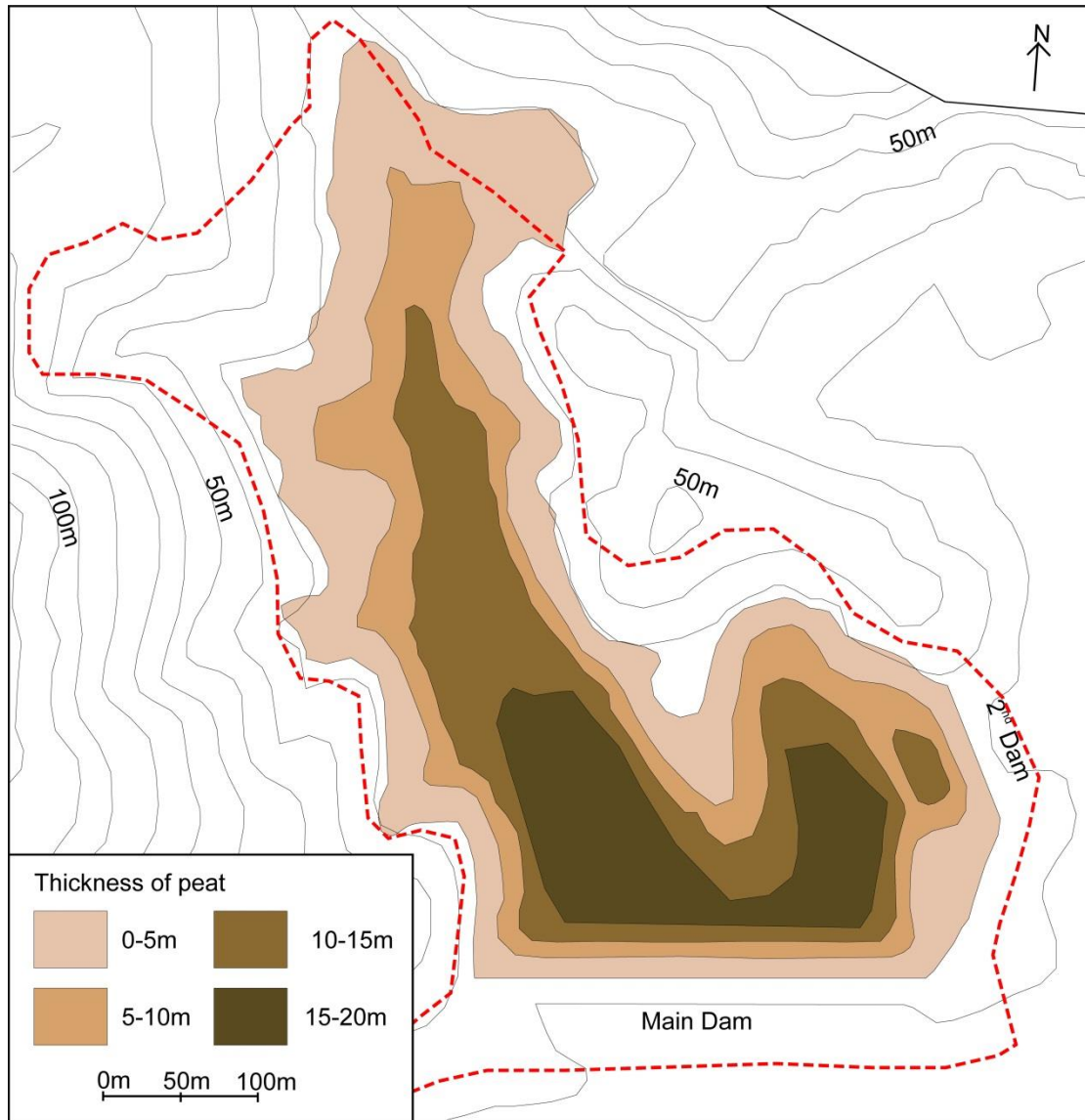


Fig. 2 Contour diagram of thickness of the peat deposited at Jiangyangfan Eco-park

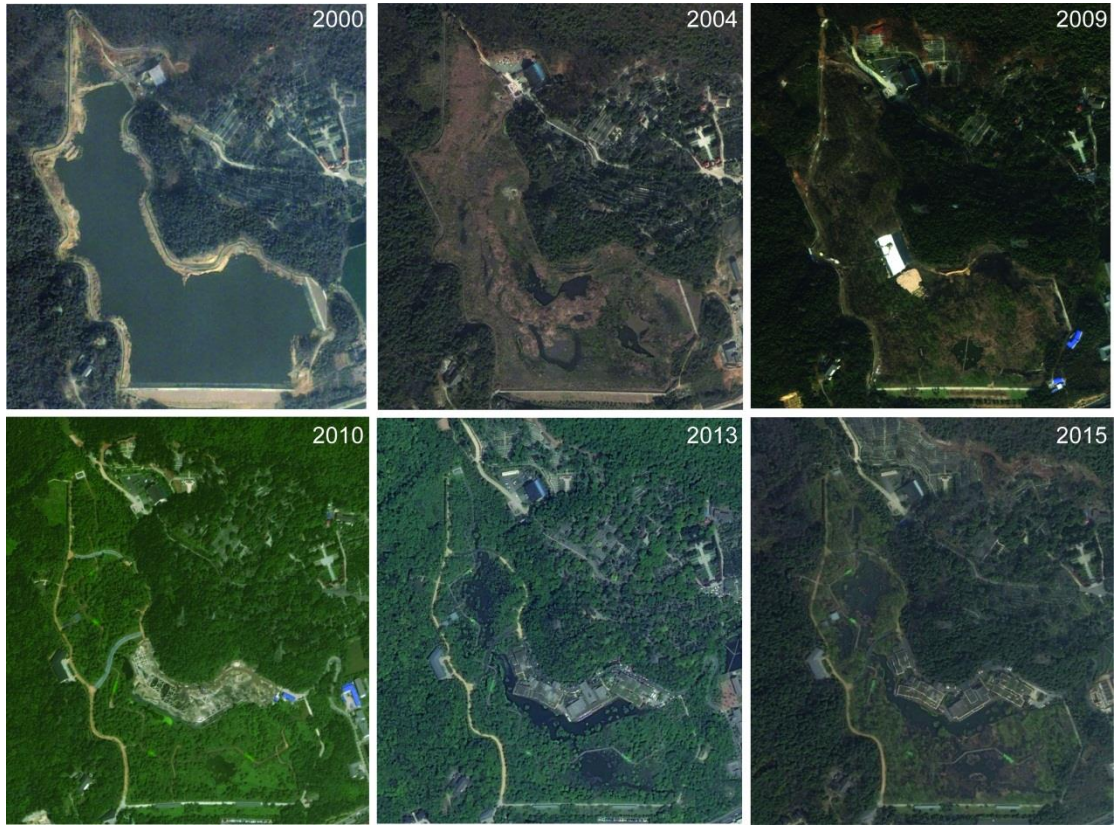


Fig. 3 Chronological aerial views of Jiangyangfan Eco-park site

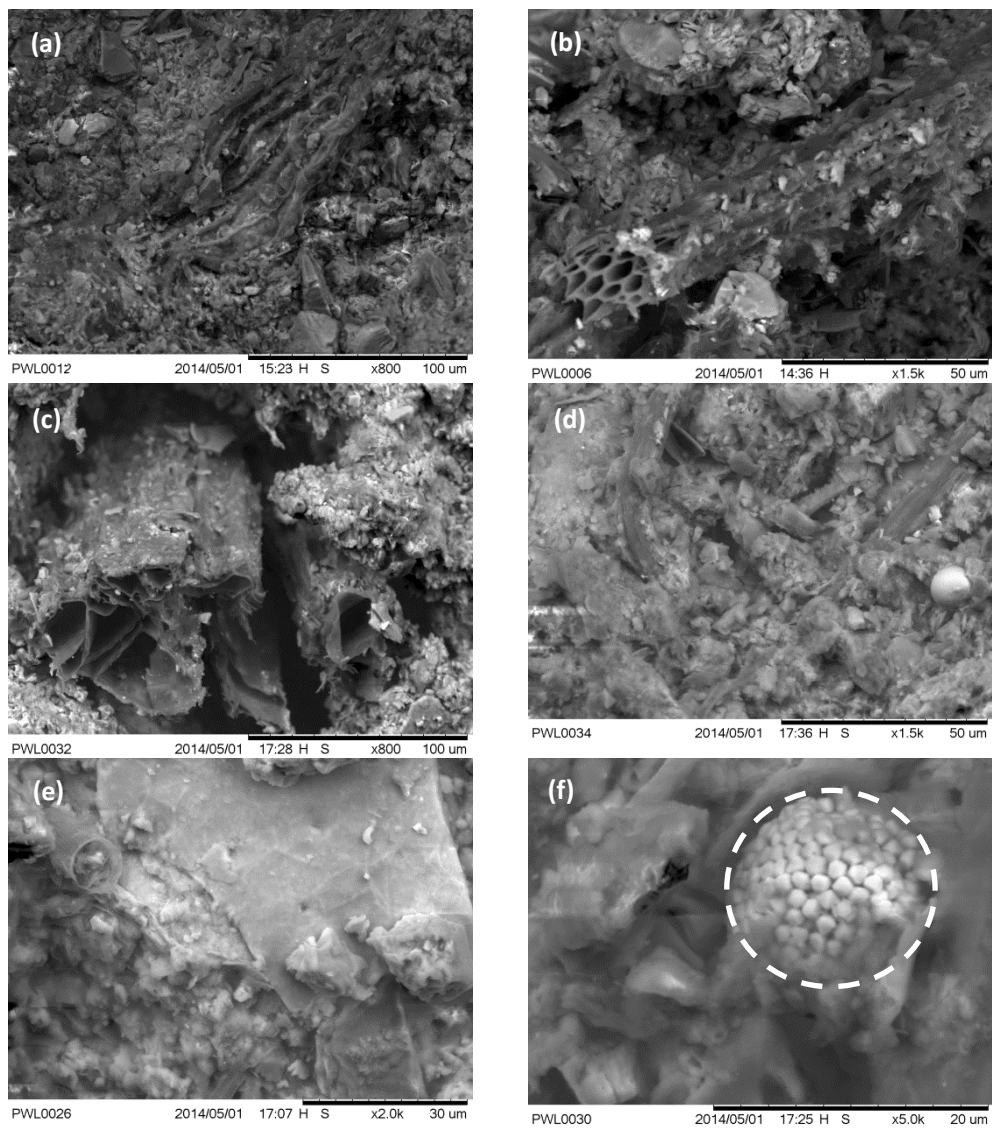


Fig. 4 Scanning electron microscope images of peat samples (a) organic fibres; (b), (c) and (d) stem structures; (e) leaves; (f) pyritic framboids

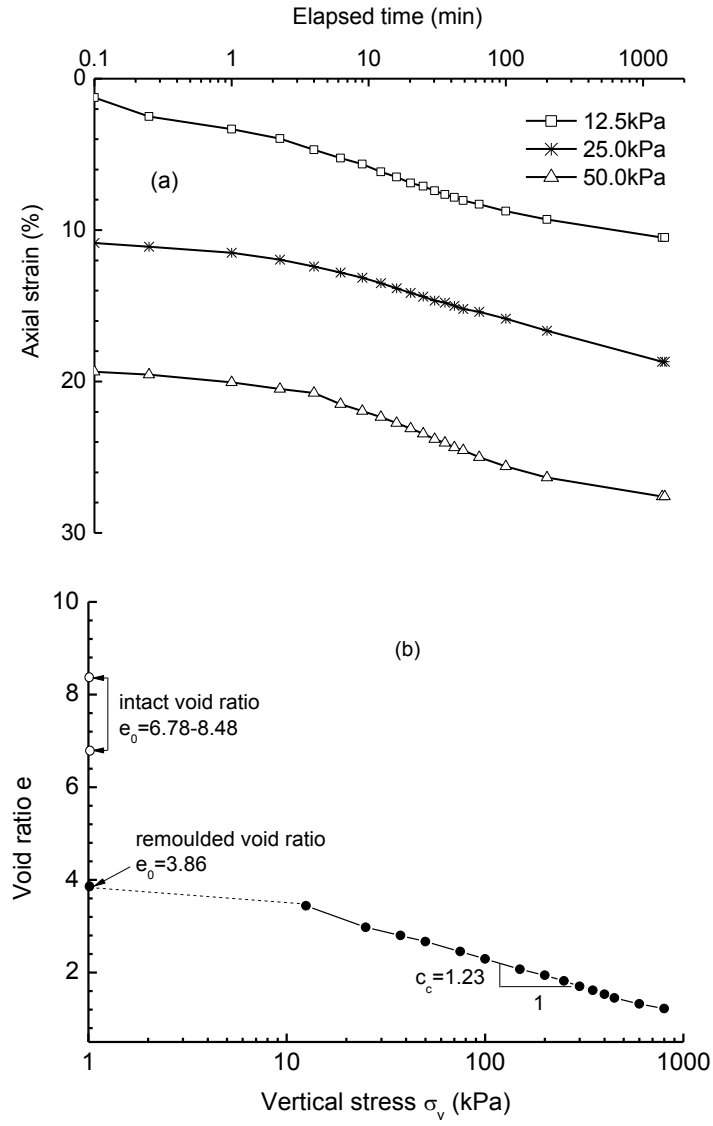


Fig. 5 One-dimensional compression of the WLP
 (a) loading increment against elapsed time; (b) e - $\log(\sigma_v)$ curve;

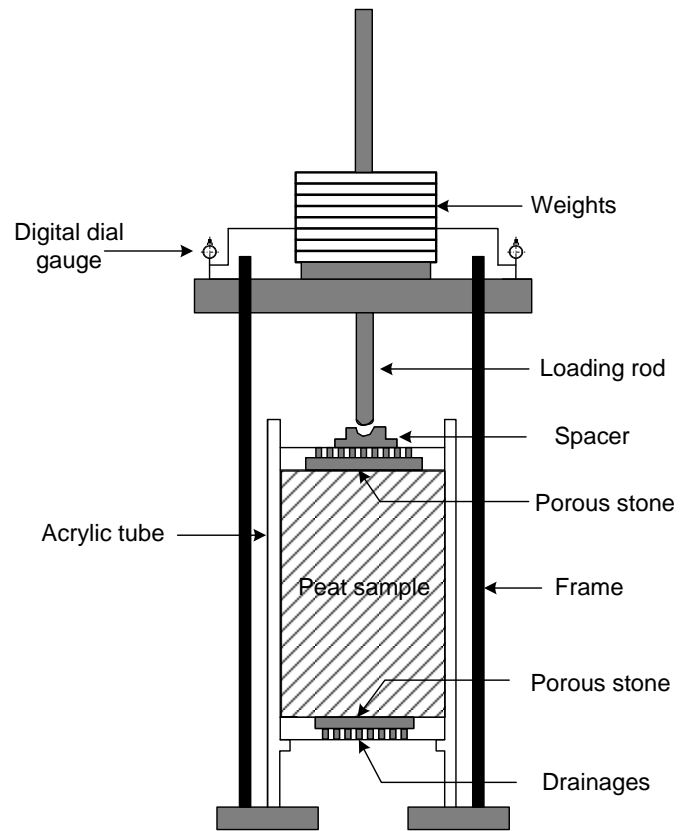


Fig. 6 Schematic drawing of the device for reconstituted sample preparation

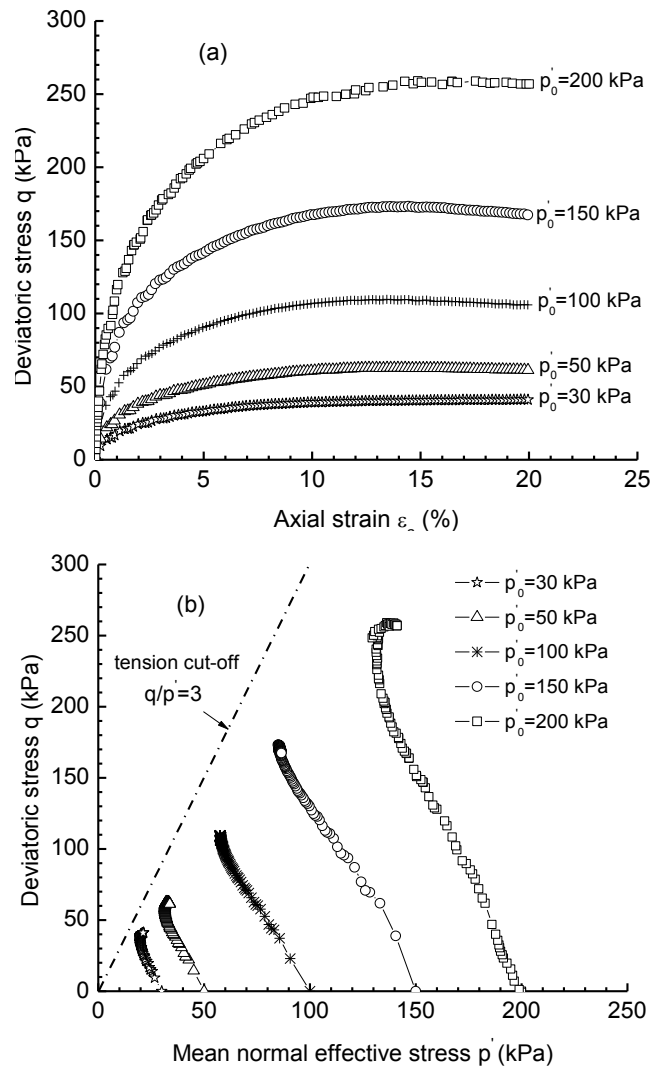


Fig. 7 Triaxial compression tests for peat (a) effective stress paths; (b) stress-strain curves

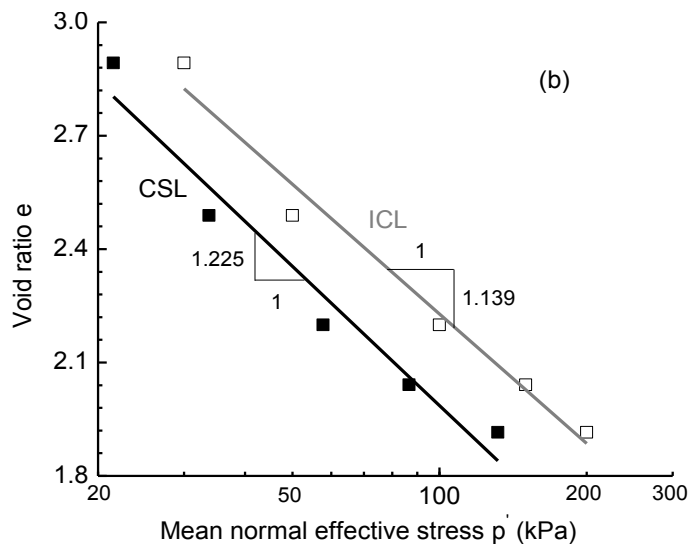
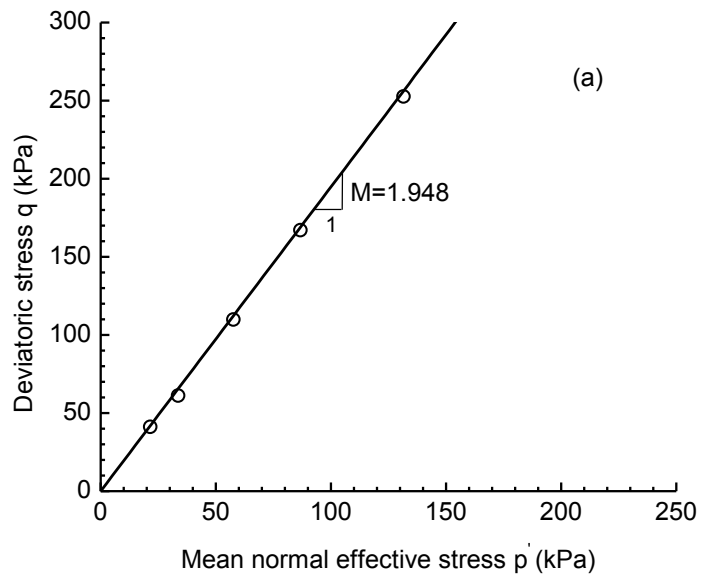


Fig. 8 Critical state line (a) q - p' plane; (b) e - $\log p'$ plane

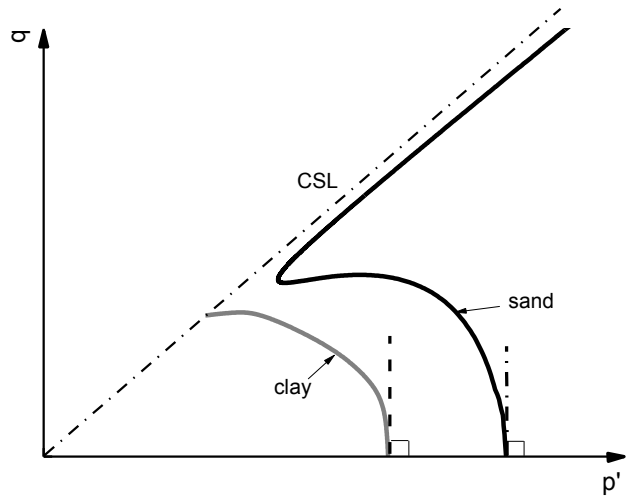


Fig. 9 Typical effective stress paths for sand and normally consolidated clay

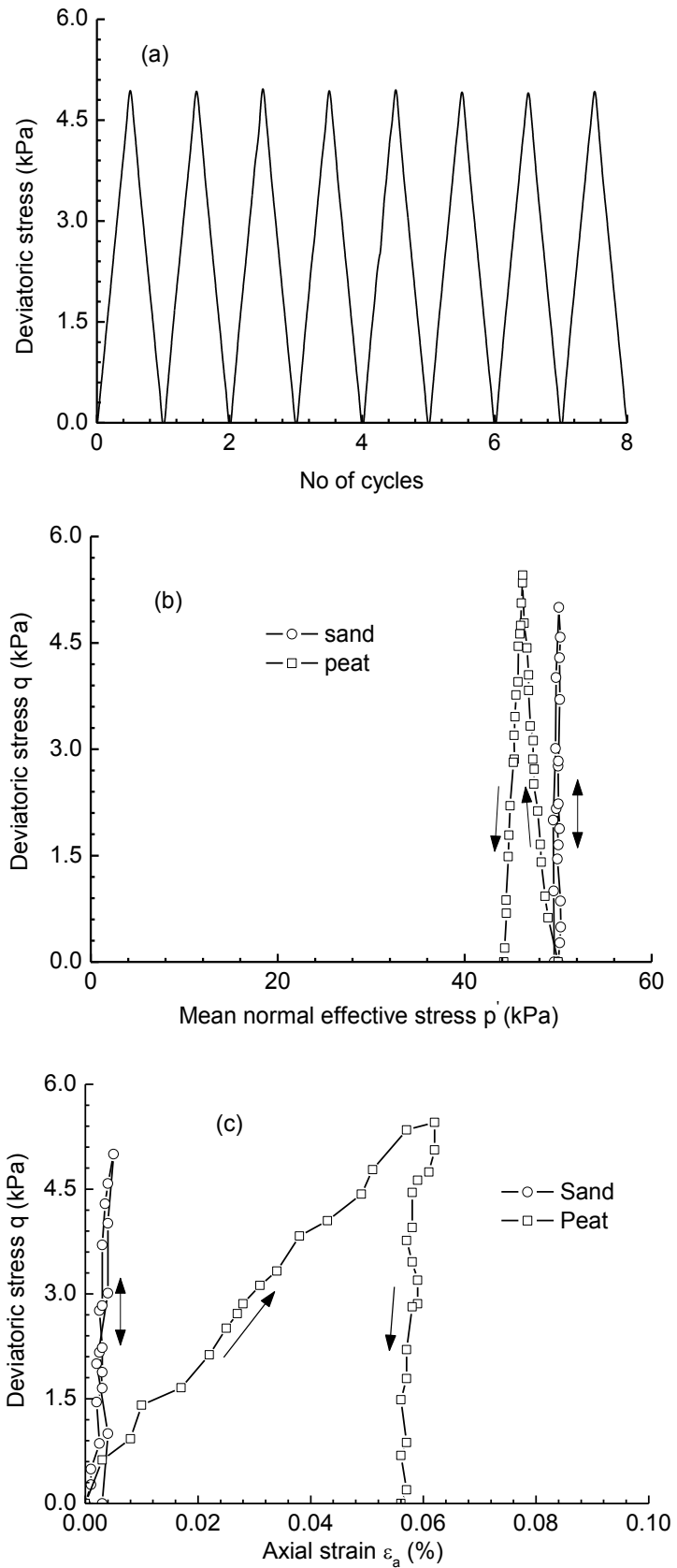


Fig. 10 Peat response under low-amplitude cyclic loading (a) cyclic deviatoric ($q_{cyc}=5$ kPa) loading; (b) 1st cycle response in q - p plane; (c) 1st cycle response in q - ϵ_a plane

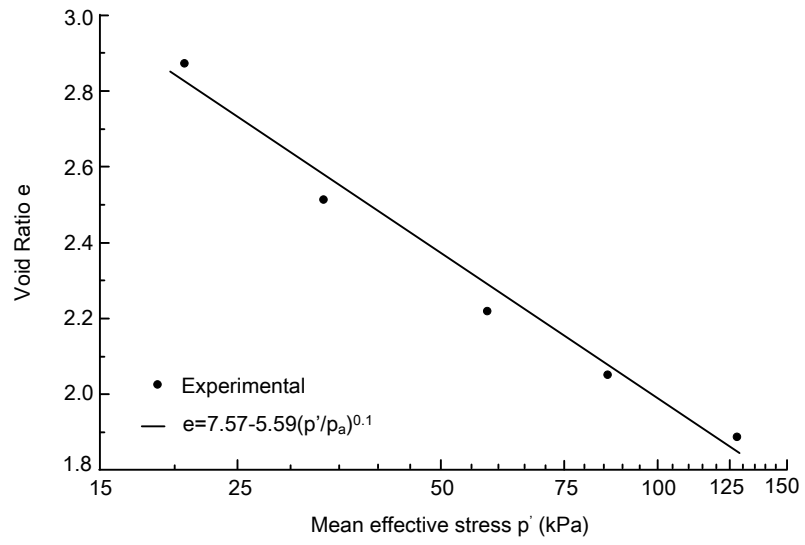


Fig. 11 Linearized critical state line for peat in the constitutive modelling

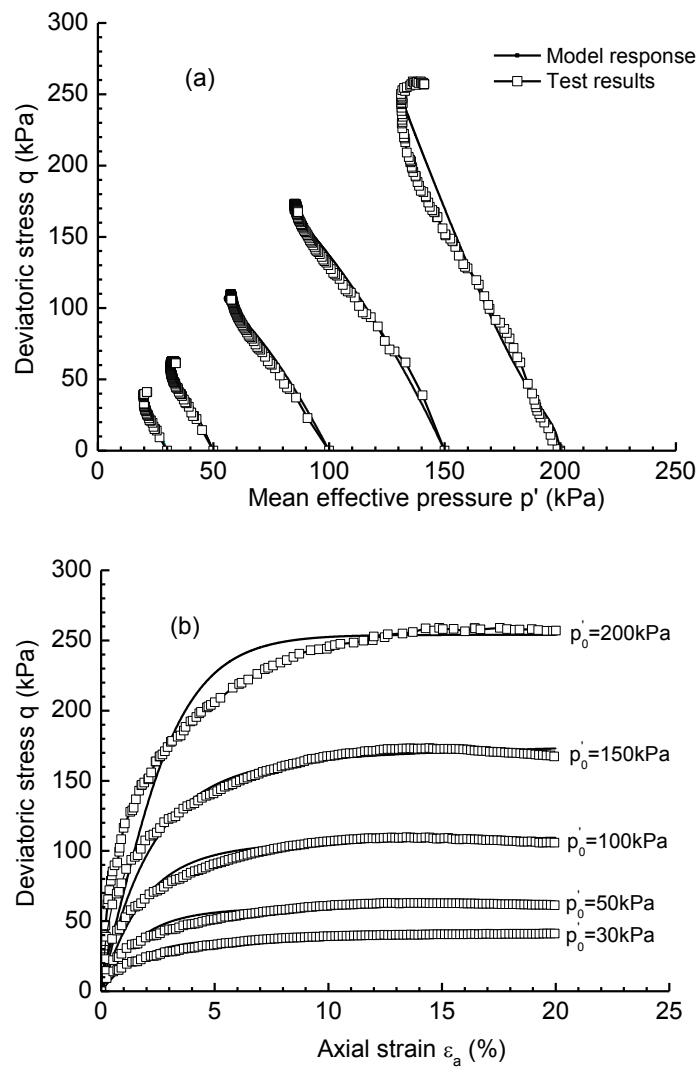


Fig. 12 Comparison between experimental results and model responses for peat
 (a) effective stress path; (b) stress-strain curve

Table 1 index properties of West Lake Peat

Natural water content w_0 (%)	Natural bulk density ρ (g/cm ³)	Reconstituted water content w_0 (%)	Specific gravity G_s	Loss on ignition N (%)	Fiber content FC (%) Retained on 63 μ m	Fiber content FC (%) Retained on 154 μ m	Acidity pH	Permeability k_v (cm/s)
320-400	1.06-1.18	182	2.12	35.0	16.1	4.3	6.4	$(2.40-1.83) \times 10^{-8}$

Table 2 Model parameters for West Lake Peat

Elastic Parameters	Critical state parameters	Dilatancy parameters	Hardening parameters
$G_0=109$ $\nu=0.209$	$M=1.948$ $e_f=7.57$ $\lambda_c=5.59$ $\xi=0.1$	$d_0=0.08$ $m=0.105$	$h_1=0.587$ $h_2=0.139$ $n=0.105$